

Magnetothermal transport in the spin-1/2 chains of copper pyrazine dinitrate

A. V. Sologubenko,¹ K. Berggold,¹ T. Lorenz,¹ A. Rosch,² E. Shimshoni,³ M. D. Phillips,⁴ and M. M. Turnbull⁴

¹*II. Physikalisches Institut, Universität zu Köln, 50937 Köln, Germany*

²*Institut für Theoretische Physik, Universität zu Köln, 50937 Köln, Germany*

³*Department of Mathematics–Physics, University of Haifa at Oranim, Tivon 36006, Israel and*

⁴*Carlson School of Chemistry and Department of Physics, Clark University, Worcester, MA 01610, USA*

(Dated: December 2, 2024)

We present experiments on the thermal transport in the spin-1/2 chain compound copper pyrazine dinitrate $\text{Cu}(\text{C}_4\text{H}_4\text{N}_2)(\text{NO}_3)_2$. The heat conductivity shows a surprisingly strong dependence on the applied magnetic field B , characterized at low temperatures by two main features. The first one appearing at low B is a characteristic dip located at $\mu_B B \sim k_B T$, that may arise from Umklapp scattering. The second one is a plateau-like feature in the quantum critical regime, $\mu_B |B - B_c| < k_B T$, where B_c is the saturation field at $T = 0$. The latter feature clearly points towards a momentum and field independent mean free path of the spin excitations, contrary to theoretical expectations.

PACS numbers: 75.40.Gb 66.70.+f, 75.47.-m

In the last decade, considerable progress has been achieved in theoretical studies of thermal transport in one-dimensional (1D) quantum spin systems (for a recent review see Ref. 1). One of the most important model systems is the Heisenberg spin $S = 1/2$ chain with isotropic antiferromagnetic interactions, described by

$$H = J \sum_i^N \mathbf{S}^i \mathbf{S}^{i+1} - g\mu_B B \sum_i^N S_z^i, \quad (1)$$

where J is the intrachain nearest-neighbor exchange and $g\mu_B$ the magnetic moment. Recently, a number of non-trivial effects were predicted for the spin thermal conductivity (κ_s) of this system in external magnetic fields B .^{2,3,4,5,6} Of particular interest is the behavior close to the saturation field $B_c = 2J/g\mu_B$, which defines a quantum critical point.⁷ Experimental information on $\kappa_s(B)$ is, however, missing because most of the known realizations of the Hamiltonian (1) have large values of the intrachain exchange constant $J/k_B \sim 100 - 1000$ K, that severely limits the region of the phase diagram accessible using standard laboratory equipment. The existing results are limited to studies of the phonon thermal conductivity $\kappa_{\text{ph}}(B, T)$ in CuGeO_3 and Yb_4As_3 ,^{8,9,10,11} and do not address the behavior of $\kappa_s(B, T)$.

Copper pyrazine dinitrate $\text{Cu}(\text{C}_4\text{H}_4\text{N}_2)(\text{NO}_3)_2$ (CuPzN) appears to be an ideal compound for the thermal conductivity experiments in magnetic field, as $J/k_B = 10.3$ K and therefore $B_c = 15.0$ T,^{12,13} which is easily accessible experimentally. CuPzN has an orthorhombic structure with lattice constants $a = 6.712$ Å, $b = 5.142$ Å, and $c = 11.73$ Å at room temperature.¹⁴ The chains of Cu^{2+} spins $S = 1/2$ run along the a axis. Inelastic neutron scattering, magnetization, and specific heat measurements have confirmed that CuPzN is very well described by the model of Eq. (1).^{12,13,15} The 1D nature of the spin interaction is reflected by a very low ordering temperature, $T_N = 0.107$ K, and therefore the ratio of interchain (J') to intrachain (J) couplings is estimated to be tiny, $|J'/J| \approx 4.4 \times 10^{-3}$.¹⁶

In this paper, we report measurements of the thermal conductivity $\kappa(B, T)$ of CuPzN in the temperature region between 0.37 and 10 K and in magnetic fields up to 17 T. The crystals of CuPzN were grown from water solution of pyrazine and Cu nitrate via slow evaporation. The crystals have right-prism shapes with the a axis of length 10 mm directed along the height of the prism. The dimensions perpendicular to the a axis are typically of the order of 0.4×0.7 mm². Thermal conductivity was measured by a standard steady-state heat-flow technique, where the temperature difference was produced by a heater attached to one end of the sample and monitored by a matched pair of RuO_2 thermometers. The temperature difference between the thermometers was of the order of 1% of the mean temperature T . In one sample the heat flux was oriented along the a axis to measure the thermal conductivity parallel to the chains (κ^{\parallel}). On another sample, the thermal transport perpendicular to the chains (κ^{\perp}) was measured. Magnetic fields were oriented parallel to the a axis.

In Fig. 1, we show the temperature dependence of κ^{\parallel} and κ^{\perp} in constant magnetic fields. The important observation is that B strongly influences κ^{\parallel} , but no significant changes of κ^{\perp} with field are observed. In CuPzN, the magnetic interaction between the spin chains is extremely weak. Therefore one expects that the heat current perpendicular to the chains is of purely phononic origin, $\kappa^{\perp} \approx \kappa_{\text{ph}}^{\perp}$, consistent with the observed absence of a significant field dependence. Along the chain direction, $\kappa^{\parallel} = \kappa_{\text{ph}}^{0\parallel} + \kappa_m$, one can separate the field-independent phononic contribution, $\kappa_{\text{ph}}^{0\parallel}(T)$, unrelated to the presence of the spin chains, from a B dependent magnetic contribution, $\kappa_m(B, T)$. Three terms contribute to $\kappa_m = \Delta\kappa_{\text{ph}}^{\parallel} + \kappa_s + \kappa_{sp}$. First, the scattering by spin excitations affects the lifetime of phonons and gives rise to a decrease $\Delta\kappa_{\text{ph}}^{\parallel}$ of the phononic thermal conductivity. Second, there is a spin contribution κ_s to the thermal transport. Finally, a spin-phonon cross term κ_{sp} describes the ‘drag’ of spin heat currents by phononic heat

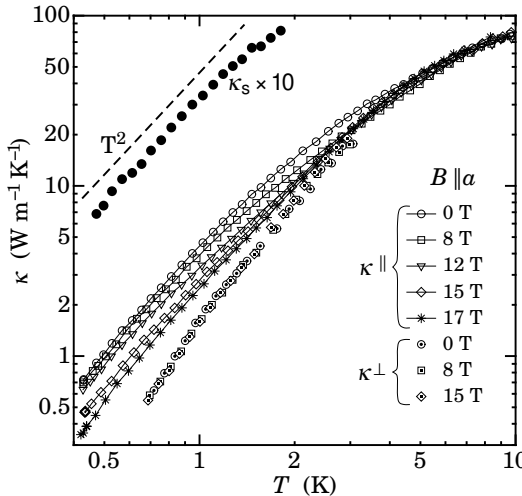


FIG. 1: The thermal conductivity of CuPzN parallel and perpendicular to the spin chains as a function of temperature in several constant magnetic fields. The solid circles correspond to the calculated zero-field spin thermal conductivity along the chains (see text).

currents (and vice versa). For constant T , the difference between the total measured $\kappa^{\parallel}(B)$ and its zero-field value $\kappa^{\parallel}(B = 0)$ allows one to extract the field dependence of the magnetic heat conductivity $\kappa_m(B, T) - \kappa_m(0, T)$.

In Fig. 2, we plot $[\kappa^{\parallel}(B) - \kappa^{\parallel}(0)]/T \approx [\kappa_m(B) - \kappa_m(0)]/T$ at several constant temperatures. Depending on T , one can distinguish two types of behavior. The crossover between these two types occurs at about 2.5 – 3 K. At low temperatures, $T \ll J/k_B$, $\kappa_m(B)$ has two main features: a decrease with a minimum at low fields and another decrease at higher fields. On top of the high-field decrease, there is a plateau-like feature in the vicinity of the critical field B_c . At high temperatures, $\kappa_m(B)$ has a simpler shape with a single minimum close to $B_c/2$. The circles in Fig. 3 show the positions of the $\kappa_m(B)$ minima. In the same figure the triangles, determined as the inflection points of $\kappa_m(B)$ curves, characterize the size of the plateau-like regions in the vicinity of B_c .

For the interpretation of these data, we first note that a spin gap $= g\mu_B(B - B_c)$ opens when B exceeds B_c .¹⁷ Therefore, for $g\mu_B(B - B_c) \gg k_B T$, both heat transport by spin excitations and phonon scattering by spin excitations should vanish. In our experiment, $\kappa_m(B)$ decreases with increasing $B > B_c$ for low $T < 2.5$ K. Thus, the observed field dependence of the thermal conductivity arises dominantly from thermal transport in the spin system and not from $\Delta\kappa_{\text{ph}}^{\parallel}$. The overall decrease of κ_m towards lower T , see Fig. 1, suggests that impurity scattering dominates spin-phonon scattering. Therefore, spin-phonon drag terms should not be important. This allows us to associate κ_m with the spin thermal conductivity κ_s . We model κ_s using a combination of a relaxation time approximation and

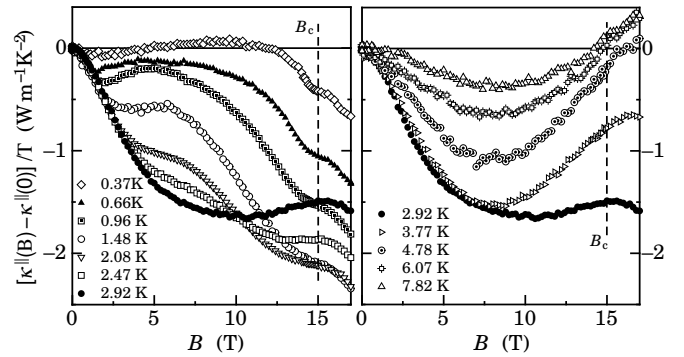


FIG. 2: Thermal conductivity parallel to the chains of CuPzN as a function of $B \parallel a$ at several fixed temperatures.

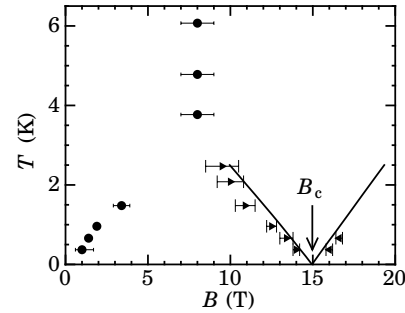


FIG. 3: A (B, T) diagram of the characteristic features of the thermal conductivity of CuPzN. The circles correspond to the minima of $\kappa_m(B)$. The triangles correspond to the inflection points of $\kappa_m(B)$ in the vicinity of B_c . The solid lines are the positions of the $\kappa_m(B)$ inflection points calculated for a constant mean free path (see text).

a mean-field theory (MFT) for the spin chain relying on mapping Eq. (1) onto a system of interacting spinless fermions via the Jordan-Wigner transformation.¹⁸ The total weight of the frequency-dependent spin thermal conductivity, $\int \kappa(\omega) d\omega$, in Heisenberg chains calculated within the MFT approach has been shown to be in reasonable agreement with exact results of the Bethe ansatz calculations.^{6,19} The fermions occupy a cosine band which, at $B = 0$, is half-filled with the chemical potential at $k_F = \pm\pi/2a$. An external magnetic field shifts the chemical potential and changes the band width. The dispersion of the fermions is

$$\varepsilon_k = -J(1 + 2\Omega) \cos(ka) - g\mu_B B + 2Jm, \quad (2)$$

where k is the wave vector and a is the distance between neighboring spins. The parameter Ω and the average local magnetization m are determined self-consistently from $\Omega = \frac{a}{\pi} \int_0^{\pi/a} \cos(ka) f_k dk$ and $m = -\frac{1}{2} + \frac{a}{\pi} \int_0^{\pi/a} f_k dk$ where $f_k = (\exp(\varepsilon_k/k_B T) + 1)^{-1}$ is the Fermi distribution

function. The spin thermal conductivity is given by

$$\kappa_s = \frac{Na}{\pi} L_2, \quad (3)$$

$$L_n = \int_0^{\pi/a} \frac{df_k}{dT} \varepsilon_k^{n-1} v_k^2 \tau_k dk, \quad (4)$$

N is the number of spins per unit volume, $v_k = d\varepsilon_k/dk$ is the velocity and τ_k is the relaxation time related to the mean free path l_k as $\tau_k = l_k/v_k$.

As discussed above, scattering by defects is expected to be the most important source of extrinsic scattering at low T . Assuming for the moment a mean free path, $l_k(B, T) = l(T)$, which is independent of both magnetic field and momentum, we can calculate $\kappa_s l^{-1}$ from Eq. (3) as a function of B and T without free parameters. For our calculations, we used the experimental values of the g -factor parallel to the a -axis $g = 2.05$ from Ref. 20 and $J/k_B = 10.3$ K from Ref. 13. The resulting $[\kappa_s(B) - \kappa_s(0)]/lT$ is shown in Fig. 4(a) for several T . The calculations obviously give correct qualitative account for the experimentally observed behavior at intermediate and high fields for all T . It reproduces the crossover from the low- T to the high- T behavior around 3 K and predicts the low- T plateau-like features at B_c with the correct width. In Fig. 3, the calculated inflection points of $\kappa_s(B)$ (solid lines) are in good agreement with the experiment. Close to the saturation field, i.e. at the quantum critical point, one finds the following scaling relation

$$\begin{aligned} \frac{\kappa_s}{Tl} &\approx \frac{Nak_B^2}{\hbar} f\left(\frac{g\mu_B(B - B_c)}{k_B T}\right), \\ f(x) &= \int_0^\infty \frac{(x-y)^2}{4\pi \cosh[(x-y)/2]^2} dy \\ &\approx \frac{\pi}{6} \begin{cases} 2 - 3e^x x^2/\pi^2 & , x \ll -1 \\ 1 - x^3/(2\pi^2) & , |x| \ll 1 \\ e^{-x}(x^2 + 2x + 2)6/\pi^2 & , x \gg 1 \end{cases} \end{aligned} \quad (5)$$

where $f(x)$ is a dimensionless scaling function independent of the precise dispersion of the spin excitations.

The comparison of the theoretical curves for various assumptions on the momentum dependence of the scattering rate, Fig. 4(b), with our experimental results, Fig. 2, clearly supports a mean free path which depends on T but *not* on momentum and magnetic field at least close to the quantum critical point. Note that close to B_c , the mapping of the spin chain to free fermions becomes exact and one may therefore hope that a simple Boltzmann description becomes asymptotically exact (if strong localization by disorder can be neglected). Here one has to emphasize, that the observation of a constant mean free path is highly surprising in a one-dimensional system. In the limit of weak disorder (small potential strength compared to T or $|B - B_c|$) the golden-rule scattering rate $1/\tau_k$ is proportional to the density of states, $1/\tau_k \propto 1/v_k$, where v_k is the velocity of the spin excitations, and therefore one gets $l_k \propto v_k^2$. Luttinger liquid corrections to

this formula are expected to vanish close to the quantum phase transition when the density of spin excitations is small. In the opposite limit of strong impurities, the spin excitations have to tunnel through the potential and the conductivity is proportional to the transmission rate, $T_k \propto v_k^2$, implying that $l \propto T_k \propto v_k^2$, as in the limit of weak disorder. However, the heat conductivity, calculated assuming $l_k \propto v_k^2$, is featureless at $B \approx B_c$, in clear disagreement with the experiment, see Fig. 4(b).

What are possible mechanisms which can lead to a constant mean free path? In the absence of inelastic scattering, interference effects lead to localization of the spin excitations but neither the observed T dependence of κ , see Fig. 1, nor the constant mean free path point towards the importance of localization effects. Nevertheless, rare defects may cut the spin chains into separate pieces of finite length. In such a situation, the effective mean free path is determined either by scattering from one spin chain to the next or – more likely – by coupling heat currents in and out of these pieces of spin chains by lattice vibrations. The first scenario naturally leads to a constant mean free path, but a theoretical prediction for the more likely second scenario is presently lacking.

Recently, several theoretical papers considered magnetothermal corrections (MTC) to the spin thermal conductivity, which should appear in a magnetic field due to a coupling of the heat and magnetization currents.^{2,4,5,6} In this case, κ_s is given, instead of Eq. (3), by^{6,19}

$$\kappa_s = \frac{Na}{\pi} \left(L_2 - \frac{L_1^2}{L_0} \right). \quad (6)$$

The second term in parentheses represents the MTC. However, in Ref. 3 it was argued that MTC are absent in macroscopic samples of real materials where the conservation of the total magnetization parallel to B is broken by spin-orbit coupling, prohibiting a piling up of magnetization. In Fig. 4(b), we show $\kappa_s(B)$ calculated within the relaxation time approximation for one temperature without (solid line) and with (dashed line) MTC. According to these calculations, MTC should completely destroy the plateau-like feature at B_c , obviously at variance with the experiment. Thus, our experiment provides strong evidence against the existence of magnetothermal corrections to the spin thermal conductivity in CuPzN.

The assumption of a constant mean free path agrees well with the experiment at intermediate and high fields but predicts a field-independent κ_s at low fields for $T \ll J/k_B$. The experiment, however, shows a low-field minimum of $\kappa_s(B)$ located approximately at $\mu_B B \sim k_B T$ for low T , see Fig. 3. This suggests strongly that the origin of this anomalous behavior is related to the physics of the half-filled band of Jordan-Wigner fermions. Only excitations in a window of width $k_B T$ around the $B = 0$ Fermi surface are able to relax their momentum to the lattice by Umklapp scattering. An explanation of the minimum might be possible along the following lines. The spin excitations which dominate the thermal transport have a typical energy of order $k_B T$, those located directly at the

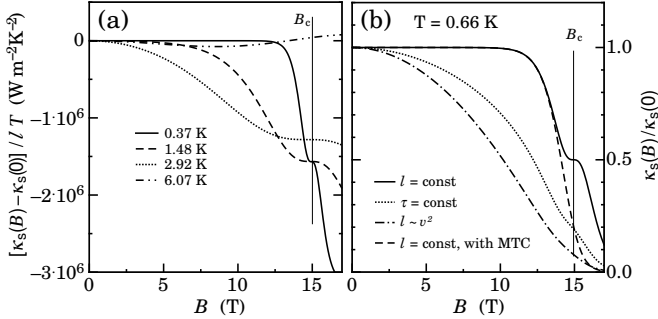


FIG. 4: (a) Spin thermal conductivity as a function of B for several T , calculated for CuPzN within a relaxation time approximation assuming a B - and momentum-independent mean free path l . (b) Spin thermal conductivity at $T = 0.66$ K, calculated under various assumptions for the mean free path (see legend), and taking into account magnetothermal corrections (dashed line). Only the model with constant l is consistent with the data.

Fermi surface with energy 0 do not contribute. Therefore, Umklapp scattering is most effective, if the excitations with energy $k_B T$ (rather than 0) have a momentum close to $\pm\pi/(2a)$, where Umklapp scattering is strongest, i.e. for $\mu_B B \sim k_B T$. Indeed, if one assumes a scattering rate with a peak at $k = \pm\pi/(2a)$, the relaxation time approximation yields a minimum in $\kappa(B)$ at the right position (not shown). An exponentially strong maximum in $\kappa(B)$ has been theoretically predicted for clean spin chains coupled to phonons in Ref. 3 as a consequence of the existence of certain approximate conservation laws. As our system is disorder dominated, we do not believe

that this mechanism is directly applicable in the present situation. A full theory of the low-field minimum should include the interplay of Umklapp, impurity and phonon scattering which is currently under investigation.

According to Eqs. (3, 5), at low T , $\kappa_s(B_c, T) \simeq \kappa_s(0, T)/2$, see Fig. 4(b). Using this, we estimate the absolute values of the zero-field spin contribution as $\kappa_s(0, T) \approx 2[\kappa(0, T) - \kappa(B_c, T)]$, which is shown in Fig. 1. It is notable that $\kappa_s \propto T^2$ implying a linear increase of the mean free path with T as $l = AT$, with $A = 1.0 \times 10^{-6}$ m/K for $T \lesssim 1.5$ K. This observation is in agreement with theoretical predictions for weakly disordered spin chains, where the linear T dependence arises from the renormalization of the impurity potentials by Luttinger liquid corrections, see e.g. Refs. 21,22.

In summary, we have experimentally established the magnetic contribution κ_m to the thermal conductivity of the $S = 1/2$ chain compound copper pyrazine dinitrate. At low temperatures, the field dependence of κ_m is characterized by two features, one at high fields in the vicinity of B_c and the other at low fields. The low-field feature remains to be explained. The high-field feature is associated to the spin thermal transport κ_s with a mean free path surprisingly weakly dependent on both field and momentum. No magnetothermal corrections to κ_s have been identified in our experiment.

Acknowledgments

We acknowledge useful discussions with P. Jung and A. K. Kolezhuk. This work was supported by the DFG through SFB 608 and by the GIF.

¹ X. Zotos, J. Phys. Soc. Jpn. Suppl. **74**, 173 (2005).
² K. Louis and C. Gros, Phys. Rev. B **67**, 224410 (2003).
³ E. Shimshoni, N. Andrei, and A. Rosch, Phys. Rev. B **68**, 104401 (2003).
⁴ K. Sakai and A. Klümper, J. Phys. Soc. Jpn. Suppl. **74**, 196 (2005).
⁵ K. Sakai and A. Klümper, J. Phys. A: Math. Gen. **36**, 11617 (2003).
⁶ F. Heidrich-Meisner, A. Honecker, and W. Brenig, Phys. Rev. B **71**, 184415 (2005).
⁷ S. Sachdev, *Quantum Phase Transitions* (Cambridge University Press, Cambridge, 1999).
⁸ Y. Ando *et al.*, Phys. Rev. B **58**, R2913 (1998).
⁹ J. Takeya *et al.*, Phys. Rev. B **63**, 214407 (2001).
¹⁰ M. Hofmann *et al.*, Physica B **312-313**, 597 (2002).
¹¹ M. Köppen *et al.*, Phys. Rev. Lett. **82**, 4548 (1999).
¹² G. Mennenga, L. J. Dejongh, W. J. Huiskamp, and J. Reedijk, J. Magn. Magn. Mater. **44**, 89 (1984).
¹³ P. R. Hammar *et al.*, Phys. Rev. B **59**, 1008 (1999).
¹⁴ A. Santoro, A. D. Mighell, and C. W. Reimann, Acta Crystallogr. B **26**, 979 (1970).
¹⁵ M. B. Stone *et al.*, Phys. Rev. Lett. **91**, 037205 (2003).
¹⁶ T. Lancaster *et al.*, Phys. Rev. B **73**, 020410(R) (2006).
¹⁷ G. Müller, H. Thomas, H. Beck, and J. C. Bonner, Phys. Rev. B **24**, 1429 (1981).
¹⁸ P. Jordan and E. Wigner, Z. Phys. **47**, 631 (1928).
¹⁹ F. Heidrich-Meisner, PhD thesis, Technische Universität Braunschweig, 2005.
²⁰ K. T. McGregor and Z. G. Soos, J. Chem. Phys. **64**, 2506 (1976).
²¹ S. Eggert and I. Affleck, Phys. Rev. B **46**, 10866 (1992).
²² A. V. Rozhkov and A. L. Chernyshev, Phys. Rev. Lett. **94**, 087201 (2005).